Appl. Phys. B (2014) 115:533–539
DOI 10.1007/s00340-013-5633-9

Applied Physics B
Lasers and Optics

Principles and calibration of collinear photofragmentation and atomic absorption spectroscopy

Tapio Sorvajärvi · Juha Toivonen

Received: 17 May 2013 / Accepted: 27 August 2013 / Published online: 15 September 2013

Abstract The kinetics of signal formation in collinear photofragmentation and atomic absorption spectroscopy (CPFAAS) are discussed, and theoretical equations describing the relation between the concentration of the target molecule and the detected atomic absorption in case of pure and impure samples are derived. The validity of the equation for pure samples is studied experimentally by comparing measured target molecule concentrations to concentrations determined using two other independent techniques. Our study shows that CPFAAS is capable of measuring target molecule concentrations from parts per billion (ppb) to hundreds of parts per million (ppm) in microsecond timescale. Moreover, the possibility to extend the dynamic range to cover eight orders of magnitude with a proper selection of fragmentation light source is discussed. The maximum deviation between the CPFAAS technique and a reference measurement technique is found to be less than 5 %. In this study, potassium chloride vapor and atomic potassium are used as a target molecule and a probed atom, respectively.

1 Introduction

Photofragmentation and fragment detection (PF/FD) techniques improve selectivity and sensitivity in gas sensing [1]. They are based on the fragmentation of the detected molecule and the sensing of the released fragment. Molecule [2], atom [3], and ion [4] fragments have been used in sensing the target molecules. Fragments are detected utilizing their emission [5–7] or absorption [8, 9] properties.

Recently, a technique called collinear photofragmentation and atomic absorption spectroscopy (CPFAAS) was demonstrated in the detection of alkali chloride vapors [10]. The technique utilizes a UV laser pulse to dissociate alkali chloride molecules to alkali and chlorine atoms, and a narrow bandwidth laser diode to monitor the concentration of the alkali atom. The collinear alignment of the two beams through the sample volume enables the detection of temporally increased alkali atom concentration within the volume determined by the UV beam. The large absorption cross-sections and the narrow absorption profiles of the alkali atoms favor their detection, also when interfering fragments, such as O_2, exist.

In this paper, a theoretical approach for signal formation in CPFAAS is discussed, and relations between detected fragment atom absorption and target molecule concentration in different conditions are derived. The theoretically derived relation for pure sample is validated by comparing KCl vapor concentrations measured with the CPFAAS technique to concentrations determined with two other independent reference techniques. The linearity of the CPFAAS technique with respect to the target molecule concentration and the absolute limits of the CPFAAS detection at low and high concentration ends are also discussed.

2 Theoretical approach

CPFAAS is based on the fragmentation of a fraction of the target molecules with a light pulse and the detection of the released fragments within the gas volume drawn by the pulse with a collinearly aligned continuous wave probe

T. Sorvajärvi (✉) · J. Toivonen
Optics Laboratory, Department of Physics, Tampere University of Technology, P.O. Box 692, 33101 Tampere, Finland
e-mail: tapio.sorvajarvi@tut.fi

beam. The probe beam consists of monochromatic light, whose wavelength is preselected to correspond to the absorption line of the probed atom fragment. The transmission of the probe beam is monitored continuously in the vicinity of the fragmentation, which enables the determination of the transmission base level I_0 at $t < 0$, the fragmentation-induced increased absorption at $t = 0$, and the recovery of the gas sample back to the thermal equilibrium at $t > 0$. Applying the Beer–Lambert law to describe the transmission of the probe beam and assuming an exponential decrease for the concentration of the produced fragments at $t > 0$, the transmission intensity I of the probe beam can be expressed as:

$$I(t) = \begin{cases} I_0 + C & t < 0 \\ I_0 \exp\left(-\alpha L_{\max} e^{(-t/\tau)}\right) + C & t \geq 0 \end{cases}, \quad (1)$$

where α $L_{\max}$ and τ are the maximum absorbance due to the fragment atoms at $t = 0$ and a time constant for the decay process, respectively. The offset parameter C is added to describe the fraction of the probing light that passes the sample without interacting with the fragments due to the misalignment of the beams or the spectral impurity of the probe beam.

The dependence of the detected quantity α $L_{\max}$ on a definable quantity target molecule concentration X_{KCl} can be studied by eliminating C and assuming that the recovery of the fragments is negligible during the excitation time, e.g., relaxation time is much longer than the excitation pulse, when the transmission intensity at $t = 0$ can be written as

$$I(t = 0) = I_0 \exp(-\alpha L_{\max}) = \exp\left(-\frac{N_K}{V_f}\sigma_K L\right), \quad (2)$$

where N_K, V_f, σ_K and L are the total number of produced fragment atoms, a volume in which the fragmentation has occurred, the absorption cross-section of the fragment atoms at the probe wavelength and sample length, respectively. N_K is directly proportional to the number of the absorbed fragmentation photons by the target molecules and can be rewritten as a relation between absorbed energy by target molecule $E^{\mathrm{abs}}_{\mathrm{KCl}}$ and the energy of a single fragmentation photon $E_{\mathrm{photon}} = hc/\lambda_f$ multiplied with the photofragmentation efficiency γ at the fragmentation wavelength

$$N_K = \gamma \frac{E^{abs}_{KCl}}{\frac{hc}{\lambda_f}} \quad (3)$$

where h, c and λ_f are Planck's constant, speed of light, and the wavelength of the fragmenting pulse, respectively. The photofragmentation efficiency depends on the target molecule and the fragmentation wavelength. For example, the photofragmentation of NO_2 produces O atoms with fragmentation efficiency of $0 \leq \gamma \leq 1$ in the vicinity of 400 nm [11], and the fragmentation of $SeBr_2$ produces Br atoms with $\gamma = 2$ in the vicinity of 350 nm [12]. Alkali chlorides are known to have $\gamma = 1$ for production of ground state alkali atoms in the vicinity of 250 nm [13].

On the other hand, total fragmentation energy absorbed by a sample is a sum of energy absorbed by the target molecule and energy lost due to other extinction mechanisms E^{ext}

$$E^{abs}_{\mathrm{KCl}} + E^{\mathrm{ext}} = E_{\mathrm{in}} - E_{\mathrm{out}}, \quad (4)$$

where E_{in} and E_{out} are the energy of the fragmentation pulse at the input and at the output of the sample, respectively. By solving $E^{\mathrm{abs}}_{\mathrm{KCl}}$ out from Eq. 3, N_K out from Eq. 2 and dividing both sides in Eq. 4 with $E_{\mathrm{in}} - E_{\mathrm{out}}$ we get:

$$R_{\mathrm{KCl}} + R_{\mathrm{other}} = 1 \left| \begin{array}{l} R_{\mathrm{KCl}} = \alpha L_{\max} \frac{hc}{\gamma \lambda_f} \frac{V_f}{\sigma_K L (E_{\mathrm{in}} - E_{\mathrm{out}})} \\ R_{\mathrm{other}} = \frac{E^{\mathrm{ext}}}{E_{\mathrm{in}} - E_{\mathrm{out}}} \end{array} \right. , \quad (5)$$

where R_{KCl} and R_{other} describe the percentages of the total absorbed fragmentation energy by target molecule absorption and by other extinction mechanisms, respectively.

In measurement conditions, where target molecule absorption is dominant extinction mechanism, i.e., sample is pure, we can approximate that $R_{\mathrm{KCl}} = 1$, which yields to

$$\begin{aligned} \alpha L_{\max} \frac{hc}{\gamma \lambda_f} \frac{V_f}{\sigma_K L} &= E_{\mathrm{in}} - E_{\mathrm{out}} \\ 1 - \alpha L_{\max} \frac{hc}{\gamma \lambda_f} \frac{V_f}{\sigma_K L E_{\mathrm{in}}} &= \frac{E_{\mathrm{out}}}{E_{\mathrm{in}}}. \end{aligned} \quad (6)$$

Recalling that the fragmentation takes place only in the volume drawn by the fragmentation pulse and assuming a flat intensity distribution for the fragmentation pulse, the volume V_f can be expressed as $V_f = A_f L$, where A_f is the cross-section area of the fragmenting pulse. Moreover, we can apply the Beer–Lambert law to describe the relation $E_{\mathrm{out}}/E_{\mathrm{in}}$, and get

$$\begin{aligned} 1 - \alpha L_{\max} \frac{hc}{\gamma \lambda_f} \frac{A_f}{\sigma_K E_{\mathrm{in}}} &= \exp(-\alpha_{\mathrm{KCl}} L) \\ 1 - \alpha L_{\max} \frac{hc}{\gamma \lambda_f} \frac{A_f}{\sigma_K E_{\mathrm{in}}} &= \exp\left(-X_{\mathrm{KCl}} \frac{N}{V} \sigma_{\mathrm{KCl}} L\right), \end{aligned} \quad (7)$$

where α_{KCl}, N/V, and σ_{KCl} are target molecule absorption coefficient, total molecule density in the sample and the absorption cross-section of the target molecule at λ_f, respectively. Finally, by applying the ideal gas law to describe molecule density and solving X_{KCl} out from Eq. 7, we get a relation

$$X_{\mathrm{KCl}} = -\ln\left(1 - \alpha L_{\max} \frac{hc}{\gamma \lambda_f} \frac{1}{\sigma_K} \frac{A_f}{E_{\mathrm{in}}}\right) \frac{kT}{p} \frac{1}{\sigma_{\mathrm{KCl}} L}, \quad (8)$$

where p, k_B and T are sample pressure, the Boltzmann constant, and sample temperature, respectively. Equation 8 describes how a measurable parameter $\propto L_{\max}$ and a measurement setup specific variable fragmentation energy density E_{in}/A_f can be used to calculate the target molecule concentration from the pure samples. Other parameters in Eq. 8 are physical constants or sample specific parameters.

In measurement conditions, where the fragmentation pulse attenuates strongly while propagating through the sample, the density of the produced fragment atoms is smaller at the end of the sample than at the beginning. The strong attenuation of the fragmentation pulse in pure samples means high target molecule concentration and is taken into account in Eq. 8 as a logarithm dependence between X_{KCl} and $\propto L_{\max}$. In impure samples, the fragmentation pulse attenuates due to multiple extinction mechanisms, e.g., absorption by target molecule, absorption by other gas components, and scattering from particles. Beer–Lambert law determines that the attenuation of the fragmentation pulse can be expressed in common case as

$$\ln\left(\frac{E_{\text{in}}}{E_{\text{out}}}\right) = \sum_{i=1}^{n} \epsilon_i L = \epsilon_{\text{tot}} L, \tag{9}$$

where ε_i and ε_{tot} are the extinction coefficient of the single extinction agent and the total extinction coefficient, respectively. In order to solve the share of the target molecule absorption out from the total extinction, we can multiply the both sides in Eq. 9 by R_{KCl} and get

$$\begin{aligned} \ln\left(\frac{E_{\text{in}}}{E_{\text{out}}}\right) R_{\text{KCl}} &= R_{\text{KCl}} \epsilon_{\text{tot}} L \\ \ln\left(\frac{E_{\text{in}}}{E_{\text{out}}}\right) R_{\text{KCl}} &= \alpha_{\text{KCl}} L. \end{aligned} \tag{10}$$

Inserting the previously presented quantities R_{KCl} and α_{KCl} to Eq. 10, we get

$$\ln\left(\frac{E_{\text{in}}}{E_{\text{out}}}\right) \alpha L_{\max} \frac{\text{hc}}{\gamma \lambda_{\text{f}}} \frac{V_{\text{f}}}{\sigma_{\text{K}} L (E_{\text{in}} - E_{\text{out}})} = \text{X}_{\text{KCl}} \frac{\text{p}}{\text{kT}} \sigma_{\text{KCl}} L. \tag{11}$$

Finally, solving X_{KCl} from Eq. 11 results

$$X_{\text{KCl}} = \alpha L_{\max} \frac{A_f}{E_{\text{in}} L} \frac{hc}{\gamma \lambda_f} \frac{kT}{p} \frac{1}{\sigma_K \sigma_{\text{KCl}}} \frac{\ln(\text{E}_{\text{in}}/\text{E}_{\text{out}})}{1 - E_{\text{out}}/E_{\text{in}}}. \tag{12}$$

Equation 12 presents a common relation between the target molecule concentration X_{KCl} in pure and impure samples, and the measured quantity $\propto L_{\max}$, the measurement setup specific variable E_{in}/A_f and the background extinction correction coefficient determined by measurable energy values E_{in} and E_{out}. Other parameters in Eq. 12 are sample dependent or physical constants. In case of small extinction, a linear assumption can be applied to the logarithm term in Eq. 12, when the correction coefficient is reduced and we get an approximation

$$X_{\text{KCl}} = \alpha L_{\max} \frac{A_f}{E_{\text{in}} L} \frac{hc}{\gamma \lambda_f} \frac{kT}{p} \frac{1}{\sigma_{\text{K}} \sigma_{\text{KCl}}}. \tag{13}$$

The same approximation is also achieved when a linear assumption is applied to Eq. 8.

We can conclude that when the change in the intensity of the fragmentation pulse through the sample is undetectable, the interfering extinction mechanisms have negligible effect to the signal formation and Eq. 13 or Eq. 8 can be applied in signal processing. In case of detectable extinction, Eq. 8 should be used, when the target molecule absorption is known to be the dominant extinction mechanism in the sample, in order to minimize measurement errors due to the fluctuations between independent detectors. Finally, Eq. 12 should be used when the content of the sample is unknown or it is known to contain many different extinction agents.

3 Experiments

The validity of the theoretical derivation in pure samples was studied experimentally using a measurement setup shown in Fig. 1. The setup allowed the comparison of CPFAAS and two reference techniques in the determination of KCl concentration from sample volume. In the CPFAAS technique, a quadrupled Nd:YAG laser (FQSS 266-200, Crylas GmBh.) emitting 1 ns pulses at a 20 Hz repetition rate at the wavelength of 266 nm was used for the fragmentation of the KCl molecules. The output beam of the fragmentation laser was expanded with a factor of 10 and then limited with an aperture having a diameter of 2.8 mm in order to achieve a flat beam profile. The energy of the pulses entering the sample was monitored with an energy meter (PD10, Ophir). The K atoms released in fragmentation were probed with a distributed feedback (DFB) laser emitting light at the wavelength of 766.5 nm (in air)

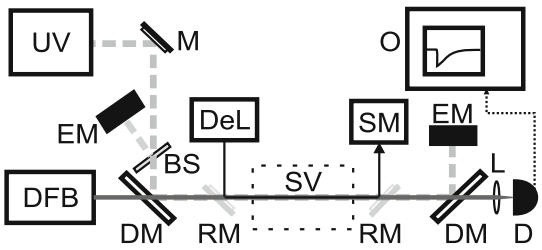

Fig. 1 Experimental setup for the detection of vaporous potassium chloride: fragmentation laser (UV); probe laser (DFB); Deuterium lamp (DeL); mirror (M); beam splitter (BS); dichroic mirror (DM); removable mirror (RM); sample volume (SV); spektrometer (SM); energy meter (EM); lens (L); detector (D); oscilloscope (O)

(Nanoplus GmbH). The wavelength of the probe laser was tuned to the absorption maximum of K vapor in a reference cell (SC-K-19 × 75-Q-W, Photonics Technologies) having inner pressure of 10^{-7} Torr and a temperature of 60 °C. The operation of the DFB laser was considered stable, as no short-term wavelength drifting compared to the K absorption maximum was observed. The UV and IR laser beams were combined on the same optical path using a dichroic mirror (FF310-Di01, Semrock). After passing the sample volume, the laser beams were separated and directed to a pulse energy meter (PE9, Ophir) and to an amplified photodiode (PDA10A, Thorlabs) with an analog bandwidth of 0–150 MHz. Probe laser transmission curves were recorded using an oscilloscope (Waverunner6000, LeCroy).

KCl sample vapor was produced by sublimating KCl powder in 80-cm-long quartz glass tube with an inner diameter of 36 mm. The powder was spread evenly at the bottom of the 50 cm long heated section of the tube. The middle point temperature of the oven ranged from 410 to 762 °C during the experiments. The ends of the quartz tube were open that led us to assume a constant pressure of 1 atm through the whole sample tube. As a first reference technique for KCl concentration, we measured the temperature profile in the oven using a K-type thermocouple and then calculated the corresponding saturated KCl vapor pressure profile through the tube using a thermochemical database (HSC 5.1, Outokumpu). The average concentration over the heated section was found to be less than half of the local maximum KCl concentration at the center of the tube.

Differential optical absorption spectroscopy (DOAS) was used as a second reference technique. DOAS applies a known reference spectrum to solve the concentration of the sample out from a measured absorption spectrum. Previously, DOAS has been applied to measure, e.g., KCl monomers at parts per million (ppm) level [14]. Instead of using KCl monomer spectrum, the combination spectrum of KCl monomers and dimers [13] was applied in this study due to the method of sample generation. DOAS measurement was done using a deuterium lamp (AvaLight-DH-S-BAL, Avantes) emitting broadband UV light and a spectrometer (AvaSpec-2048, Avantes). The broadband light beam was aligned on the same optical path with CPFAAS beams using removable mirrors. The DOAS measurements were done after each CPFAAS measurement in order to get a reference from same sample conditions. DOAS spectra were measured using 300 ms exposure time and were repeated 10 times at every temperature.

4 Results

Three CPFAAS transmission curves and their curve fittings according to Eq. 1 are presented in Fig. 2. The transmission curves were measured through the measurement cell having middle point temperatures and corresponding to calculated KCl equilibrium concentrations of (a) 456 °C and 3.8 ppb, (b) 534 °C and 126 ppb, and (c) 762 °C and 155 ppm. The signals were excited using UV pulse energies of 16μJ in measurements (a) and (b), and 1.6 μJ in measurement (c). Curve fittings yielded (a) $\alpha\ L_{\max} = 0.0056$ and $\tau = 28$ ns (b) $\alpha\ L_{\max} = 0.17$ and $\tau = 42$ ns (c) $\alpha\ L_{\max} = 13$ and $\tau = 82$ ns. Offset parameter C was determined to be 6 % of I_0 in each measurement according to transmission curve measured from KCl concentration of 155 ppm.

The fitting function showed good correspondence to the observed transmission curves in all measured conditions. The relation $\alpha\ L_{\max}/E_0$ increased with respect to the KCl concentration as was expected in Eq. 8. The relaxation time constant τ became longer when the sample temperature was increased. A similar behavior between elevated temperature and K atom decay time in O_2-rich conditions has been previously reported by Husain et al. [15]. The amount of produced K atoms was found to have negligible effect to τ when measuring transmission curve in similar condition with different E_{in} values. The oscillation observed in the vicinity of the fragmentation occurred at the frequency of the analog bandwidth limit of the used amplified photodiode. The oscillations had negligible effect to the curve fittings due to their periodic behavior and short occurrence time.

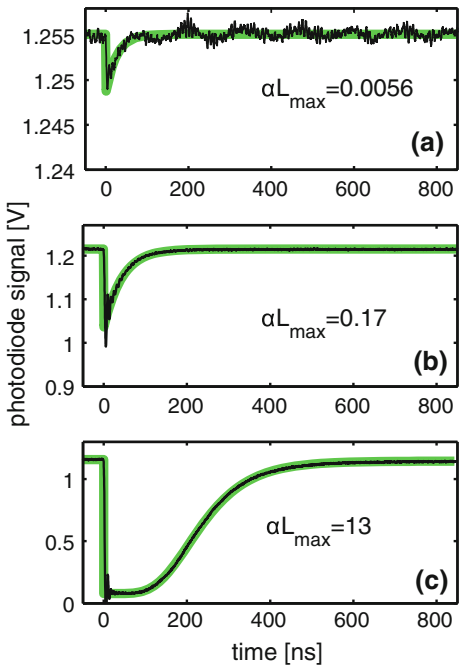

Fig. 2 Three example signals and their *curve* fittings measured from KCl equilibrium concentrations of **a** 3.8 ppb, **b** 126 ppb and **c** 155 ppm using UV pulse energies of 16, 16, and 1.6 μJ, respectively

Table 1 Variables used to calculate KCl concentrations in CPFAAS technique

Variable	Value
σ_{KCl}	0.74×10^{-21} m^2 [13]
σ_K	1.15×10^{-16} m^2
A	6.16×10^{-6} m^2
E_p	16 μJ, 1.6 μJ[a]
L	0.50 m
γ	1 [13]

[a] Lower pulse energies were used when KCl concentration was 0.4 ppm or higher in order to avoid signal saturation

In the previous chapter 2, the relation between observed $\propto L_{\max}$ and target molecule was discussed in pure an impure samples. In this study, the only extinction agent for the fragmentation pulse is KCl vapor and, therefore, Eq. 8 is applied in following calculations. The equation includes physical constants and measurement setup dependent variables. The variable values used in these experiments are presented in Table 1. The absorption cross-section of the K atom fragments at their probing wavelength was determined by utilizing the lineshape of the K atom fragments, having linewidth of 15.7 pm, determined previously [10] and the Einstein coefficient [16] for the used $4^2S_{1/2} - 4^2P_{3/2}$ electron transition. The probing wavelength was measured to be 4 pm off from the peak absorption of K fragments due to the different conditions between the reference cell and the sample cell. 4 pm offset yielded 20 % reduction to σ_K when compared to its peak value. The fragmentation pulse energies were decreased at the temperatures of $T \geq 566$ °C corresponding to the calculated equilibrium concentration of $X_{\mathrm{KCl}} \geq 0.4$ ppm in order to avoid signal saturation during the comparison measurements done with the DOAS technique. The signal saturation refers in this study to the broadening of the recovering transmission tail outside the measurement window.

KCl concentrations determined using CPFAAS technique, i.e., curve fitting parameter $\propto L_{max}$ and Eq. 8, are compared to values measured using DOAS in Fig. 3. The presented values are the averages of 10 individual measurements and the errorbars correspond to their +/- standard deviations. The standard deviation of the KCl concentrations determined by using the CPFAAS technique was smaller than 2 % of average values in all presented conditions and are indistinguishable in Fig. 3.

DOAS and CPFAAS techniques were found to result similar KCl concentration values over the measured concentration range. The measurement range was limited at the low concentration end by the sensitivity of DOAS technique and at the high concentration end by the instability of the sample vapor due to the partial melting of the KCl powder. The good correspondence between the DOAS technique and the CPFAAS technique showing less than 5 % mutual variation validates the theoretically derived Eq. 8 within the measured concentration range.

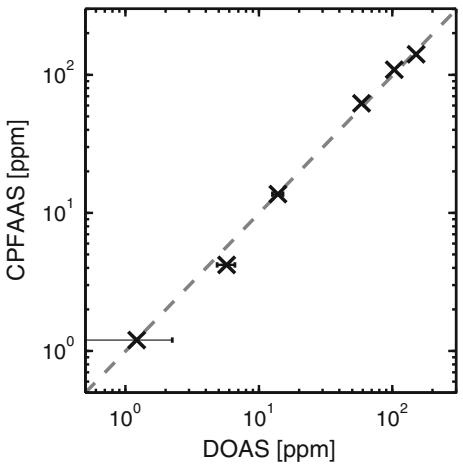

Fig. 3 Comparison between KCl concentrations measured using DOAS and CPFAAS techniques. *Dashed line* having a slope of one indicates ideal correspondence

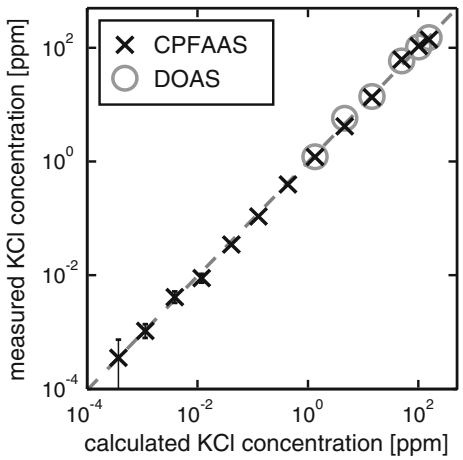

Fig. 4 Comparison between calculated equilibrium KCl concentrations and KCl concentration measured using CPFAAS and DOAS techniques. The *dashed line* having a slope of one is added to the figure to emphasize the ideal correspondence between the techniques

The linearity of CPFAAS at sub-ppm concentrations was studied by comparing the measured values to the calculated equilibrium concentrations. The equilibrium calculations were first shown to result reasonable concentrations by comparing the calculated values to the two used measurement techniques at concentrations of $X_{\mathrm{KCl}} > 1$ ppm. The comparison between the high concentration values showed that the equilibrium calculations result reasonable values and, therefore, they could be used as a reference for CPFAAS also at low concentrations. The comparison

between equilibrium calculations and CPFAAS in a concentration range of 0.4 ppb–150 ppm is shown in Fig. 4. Also, the previously presented values measured with DOAS are added to Fig. 4 as circles to show the similarity of the results. The X_{KCl} values determined with CPFAAS are averages of 10 measurements in which 10 single transmission curves were averaged before using the curve fitting tool. Error bars correspond to the ±standard deviations of the 10 single KCl concentration value at every measurement point.

An ideal correspondence line having slope of one was added to Fig. 4 in order to emphasize the differences between the KCl concentrations determined with the three different techniques. The difference between KCl concentrations determined using CPFAAS and the equilibrium calculations was less than 20 % throughout the whole measurement range. The observed fluctuation between the measured and the calculated concentrations is reasonable, especially when taking into account the possible temperature fluctuations in the sample cell due to the open ends. The 20 % change in equilibrium concentration corresponds to the temperature change of 5 °C.

The experimental results showed that the assumed CPFAAS curve shape fits well with the measured curves, and the technique can be used to determine the concentration of the sample with a good accuracy without the need for a separate calibration. The absorption dip in the non-averaged single CPFAAS transmission curves could be obtained from sample having KCl concentration of 1 ppb, which enables fast and sensitive diagnostics in microsecond timescale. The CPFAAS technique was also shown to provide at least 5 orders of magnitude dynamic range with linear response respect to the sample concentration. The theoretical saturation limit of the technique is achieved when the whole fragmentation pulse is absorbed to the sample. Assuming the minimum detectable transmissivity of the pulse is 1/1,000, we get a saturation limit of 2,500 ppm for KCl with the used measurement arrangement. At the low concentration end, the absolute detection limit is achieved when the fragmentation pulse starts to saturate the target gas absorption and $\propto L_{max}$ is indistinguishable from the detector noise. In a previous study, it was shown that the absorption of KCl is linear up to 100 μJ excitation energy when the diameter of the UV beam is 1 mm^2 and the fragmentation wavelength is 245 nm [17]. Scaling these saturation values to the values used in this study, it is found that the detection limit could still be improved with a factor of 100 by properly selecting of the fragmentation light source. According to these estimations, it is possible to achieve 8 orders of magnitude dynamic range in the detection of KCl by tuning the fragmentation pulse energy.

5 Conclusions

The principles and the signal formation in the CPFAAS technique were discussed, and the theoretical relations between absorption by the fragment atoms and the target molecule concentration were introduced in different measurement conditions. The theoretical treatment of pure samples was verified with experiments including the comparison between the assumed and the measured shape of the probe laser transmission curve in the vicinity of the fragmentation, and with the comparison between sample concentrations determined using CPFAAS and two independent reference techniques. The sample gas in these experiments was KCl vapor that was produced by sublimating KCl powder in a quartz glass tube using temperatures from 410 to 762 °C.

The demonstrated linear response over five orders of magnitude and discussed achievable dynamic range of eight orders of magnitude are important properties when strongly fluctuating samples are analyzed. Moreover, the capability of detecting 1 ppb sample concentration within 1 μs provides an excellent time resolution. CPFAAS can be applied to measure target molecule concentrations from small laboratory scale samples due to its good sensitivity and large sample volumes due to its immunity against strong attenuation of the fragmentation pulse. The absolute limits for detection are the electrical noise of the detector at the low concentration end and the non-detectable transmissivity of the fragmentation pulse at the high concentration end.

Acknowledgments This work has been partly carried out within the consortium FUSEC (2011–2014) with support from National Technology Agency of Finland (Tekes), Andritz Oy, Metso Power Oy, Foster Wheeler Energia Oy, UPM-Kymmene Oyj, Clyde Bergemann GmbH, International Paper Inc. and Top Analytica Oy Ab. T. Sorvajärvi acknowledges support from the graduate school of Tampere University of Technology.

References

1. J. Simeonsson, R. Sausa, TrAC Trends Anal. Chem. **17**(8), 542 (1998)
2. J. Simeonsson, R. Sausa, Appl. Spectrosc. **50**(10), 1277 (1996)
3. R. Oldenborg, S. Baughcum, Anal. Chem. **58**(7), 1430 (1986)
4. O. Johansson, J. Bood, M. Alden, U. Lindblad, Appl. Spectrosc. **62**(1), 66 (2008)
5. J. Silver, D. Worsnop, A. Freedman, C. Kolb, J. Chem. Phys. **84**, 4378 (1986)
6. D.E. Self, J.M. Plane, Phys. Chem. Chem. Phys. **4**(1), 16 (2002)

7. C. Erbel, M. Mayerhofer, P. Monkhouse, M. Gaderer, H. Spliethoff, Proc. Combust. Inst. **34**, 2331 (2013)
8. S. Edelstein, P. Davidovits, J. Chem. Phys. **55**, 5164 (1971)
9. D. Ehrlich, R. Osgood Jr, IEEE J. Quantum Electron. **16**(3), 257 (2002)
10. T. Sorvajärvi, J. Saarela, J. Toivonen, Opt. Lett. **37**(19), 4011 (2012)
11. C.M. Roehl, J.J. Orlando, G.S. Tyndall, R.E. Shetter, G.J. Vazquez, C.A. Cantrell, J.G. Calvert, J. Phys. Chem. **98**(32), 7837 (1994)
12. R. Samuel, Rev. Mod. Phys. **18**(1), 103 (1946)
13. P. Davidovits, D.C. Brodhead, J. Chem. Phys. **46**(8), 2968 (1967)
14. C. Forsberg, M. Broström, R. Backman, E. Edvardsson, S. Badiei, M. Berg, H. Kassman, Rev. Sci. Instrum. **80**, 023104 (2009)
15. D. Husain, Y. Lee, P. Marshall, Combust. Flame **68**(2), 143 (1987)
16. D. Morton, Astrophys. J. Suppl. Ser. **149**(1), 205 (2003)
17. T. Sorvajärvi, A. Manninen, J. Toivonen, J. Saarela, R. Hernberg, Rev. Sci. Instrum. **80**, 123103 (2009)